분자의학 및 바이오제약 석사학위 논문

Monitoring of intravenously injected exosome-mimetic nanovesicles labeled with ^{99m}Tc-HMPAO by small animal SPECT/CT imaging

소동물 SPECT/CT를 이용한 ^{99m}Tc-HMPAO을 표지한

엑소좀 모방 나노소포체의 생체 내 분포 모니터링

2014년 8 월

서울대학교 융합과학기술대학원

분자의학 및 바이오제약학과

유 민 영

Contents

Abstract

Monitoring of intravenously injected exosome-mimetic nanovesicles labeled with ^{99m}Tc-HMPAO by small animal SPECT/CT imaging

Min Young Yoo

WCU, Department of Molecular Medicine and Biopharmaceutical Science,

The Graduate School of Convergence Science and Technology,

Seoul National University

Purpose:

The exosome-mimetic nanovesicles (NVs), which are developed as an alternative to exosome, were recently reported as a potential drug delivery vehicle. It is crucial to visualize the *in vivo* distribution of NVs as a drug nanocarrier for better understanding the *in vivo* fate of NVs. Until recently, fluorescence-based *in vivo* imaging approach was examined for evaluating *in vivo* behavior of NVs. However, this fluorescence method has intrinsic limitation hampers to accelerate human application. In this study, we successfully labeled macrophage-derived NVs with the lipophilic radiotracer ^{99m}Tc-hexamethylpropyleneamineoxime (HMAPO) with a simple labeling method and examined the quantitative *in vivo* distribution of

^{99m}Tc-HMPAO labeled NVs through SPECT/CT imaging in living mice.

Methods:

Nanovesicles (NVs) were produced from mouse RAW 264.7 macrophages. After break down of the macrophages, serial extrusion was performed with diminishing pore sizes (10, 5, and 1 μm). NVs labeling was performed by 1 hour incubation of ^{99m}Tc-HMPAO in room temperature, followed by removal of ^{99m}Tc-HMAPO using PD-10 column or exosome spin column (MW30000). The serum stability test was performed on human serum at the time point of 10 min, 30 min, 1 h and 3 h after radiolabeling. To evaluate *in vivo* biodistribution of intravenously injected NVs in mouse, SPECT/CT scan was serially done at 30 min, 3 h, and 5 h after ^{99m}Tc-HMPAO labeled NVs and ^{99m}Tc-HMPAO injection.

Results:

One hour after incubation of NVs with ^{99m}Tc-HMPAO in room temperature followed by elution over PD-10 column or centrifugation with exosome spin column, the labeling efficiency showed comparable result of 99.64% and 93.73 ± 5.38%, respectively. Even though ^{99m}Tc-HMPAO labeled NVs were relatively stable in serum condition, showing more than 90% until 30 min, serum stability was decreased to the 70% after 1 h incubation. *In vivo* SPECT/CT imaging exhibited totally different pattern between labeled NVs and ^{99m}Tc-HMPAO,

showing that radioactivity of labeled NVs in the liver was much higher than that of ^{99m}Tc-HMPAO in 30 min and 3 h image. However, minor radioactivity was also observed in heart and salivary glands in labeled NVs group. The quantitative ROI measurement showed that the liver and spleen uptake was seen up to 50% of injected dose.

Conclusion:

In this study, we examined the quantitative *in vivo* distribution of ^{99m}Tc-HMPAO labeled NVs through SPECT/CT imaging in living mice. We expect that the radiolabeled NVs can provide useful information to understand *in vivo* behavior for exosome-based drug delivery.

Keywords: Exosome, ^{99m}Tc-HMPAO, Radiolabeling

Student number: 2012-24149

List of Figures

Introduction

Exosome is nanosized endogenous vesicle which delivers biological information between cells (1). The ability of exosome that carries genetic and proteomic information makes it play a role as nature vehicles for cell to cell interaction (2). Because of their nature stability in blood, immune-tolerance and nature targeting capacity, exosome has received a lot of attention as a stable nanocarrier of drugs (3). Ohno et al. reported that exosome can be used to target cancerous tissue by transporting nucleic acid (4). However, there are still several limitations for using exosome as a practical drug delivery vehicle. Firstly, quantity of exosome obtained by conventional method is very small (0.3 to 0.5 μg of exosome per 10^6 dendritic cells in 24 h) (5) and the course of purification of exosome is complicated (6). Recently, Jang at al. developed exosome mimetic bioinspired nanovesicles for alternative to exosome (7). This exosome-mimetic nanovesicles (NVs) are produced by serial extrusion of parent cells and show similar characteristics with original exosome in size, morphology, and protein contents. And the yield of NVs is 100 folds higher than that of natural exosome (7), they also reported that they successfully used exosome mimetic nanovesicle as a doxorubicin delivery vehicle to tumor. Second, the targeting capacity of exosome or cell derived membrane vesicles are different depending on their parent cell (3). Therefore, the biodistribution and targeting capacity of exosome should be

evaluated for each cell type before clinical use. To date, the fluorescence imaging is the most common way to evaluate biodistribution or targeting capacity of cell derived membrane vesicles (8, 9). Although the fluorescence imaging is a good tool for *in vitro* and *in vivo* imaging, it is unsuited for *in vivo* distribution study, because of its several weak points such as difficulty of quantification, the poor tissue penetration depth and non-specific autofluorescence. Radionuclide imaging is suitable for *in vivo* imaging, because radiation emitted by radionuclide has excellent penetration depth with the merit of quantification. Thus the radionuclide imaging modality has been widely used for evaluation of nanoparticles *in vivo* biodistribution (10, 11).

In this study, ^{99m}Tc-HMPAO (hexamethylpropylene-amineoxime) was used for radiolabeling of NVs to examine *in vivo* distribution of exosome-mimetic nanovesicles. ^{99m}Tc-HMPAO has been used for brain perfusion imaging and for mammalian cell labeling. Especially, ^{99m}Tc-HMPAO labeled WBC has been used for inflammation imaging in clinic without any adverse reaction (12, 13). The trapping mechanism of ^{99m}Tc-HMPAO trapped in mammalian cells with ^{99m}Tc-HMPAO is the reaction of sulfhydryl groups of the glutathione encapsulated in cells which become hydrophilic compounds (Fig. 1). Also, it was reported that liposome contained glutathione was successfully labeled with ^{99m}Tc-HMPAO (14).

The purpose of this study is to establish the simple radiolabeling procedure for

exosome-mimetic nanovesicles with ^{99m}Tc-HMPAO, and evaluate *in vivo* distribution of ^{99m}Tc-HMPAO labeled NVs using SPECT/CT imaging technique.

Methods and materials

Cell culture

The mouse macrophage cell line Raw 264.7 cells were cultured Dulbecco's Modified Eagle Medium supplemented with 10% FBS and 1% antibiotics. All cells without contamination were cultured at 37℃ in a 5% CO2 humidified incubator. Cell culture reagents were from Gibco-BRL.

Preparation of exosome-mimetic nanovesicles (NVs)

Raw 264.7 cells were suspended in phosphate-buffered saline (PBS) at a $5x10^6$ cells/mL concentration. Sequential extrusion of cell suspension was performed through 10, 5, and 1 μ*m* polycarbonate membrane filters (Whatman) using amini-extruder (Avanti Polar Lipids). 50% iodixanol (Axis-Shield PoC AS) overlaid with 10% iodixanol was placed at the bottom of an ultracentrifuge tube, for step gradient. After the extruded samples placed on 10% iodixanol, ultracentrifuged at 100000g for 2 h at 4℃. NVs were acquired from the 50 % and 10 % iodixanol layers interface. After NVs production, nanovesicles were stored as a stock in freezer at -20℃ prior to use.

Radiolabeling nanovesicles with ^{99m}Tc-HMPAO

The commercially available kit of HMPAO was labeled with $^{99m}TcO_4^-$ without stabilizer. The NVs (30 μg/100 μL - 90 μg/300 μL) were incubated for 60 min with prepared 185 - 370 MBq of ^{99m}Tc-HMPAO at room temperature. During the incubation, the tube was slowly mixed until the end of labeling.

Separation of ^{99m}Tc-HMPAO labeled NVs from $^{99m}TcO_4^-$ and ^{99m}Tc-HMPAO

Two different methods were used for removing unlabeled $^{99m}TcO_4^-$ or ^{99m}Tc-HMPAO from ^{99m}Tc-HMPAO labeled NVs. Elution over desalting column (PD-10, GE Healthcare, Milwaukee, WI, USA) or centrifugation with exosome spin column. Elution was performed over PD-10 colum eluted with 0.9% w/v NaCl solution. The eluent was collected in test tubes of 0.5 mL portions. And radiochemical purity were measured by instant thin-layer chromatography (ITLC) using Whatman no. 1 paper and 0.9% w/v NaCl solution as an eluent for each column.

The other isolation method, centrifugation was done with exosome spin column (MW30000, Invitrogen, USA). After hydration of column with 650 μL of 0.9% w/v NaCl solution, excess interstitial fluid was removed by spin the column at 750xg for 2min. And NVs with ^{99m}Tc-HMPAO suspension was centrifuged at 750xg for 2min at room temperature. After centrifugation, radiochemical purity was also investigated with ITLC using Whatman no. 1 paper. On ITLC, the NVs remained at

the origin site, while both free $^{99m}TcO4^-$ or ^{99m}Tc-HMPAO move together with the solvent. Results are expressed as percentage of count of ^{99m}Tc-HMPAO labeled NVs / Total count activity.

Size distribution of NVs

Average diameter of unlabeled nanovesicles (NVs) and ^{99m}Tc-HMPAO labeled NVs were investigated with dynamic light scattering (DLS).

The serum stability of ^{99m}Tc-HMPAO labeled NVs

100 μL preparations of NVs were radiolabeled with ^{99m}Tc-HMPAO in the manner of described previously. After removal of free ^{99m}Tc-HMPAO by centrifugation with exosome spin column, the serum stability of labeled NVs was investigated. 100 μL of ^{99m}Tc-HMPAO labeled NVs were added to 900μL of freshly prepared human serum and incubated at room temperature. 20 μL aliquots of the incubations were taken for the following time points: 10, 30, 60, and 180 min. ITLC was performed for each aliquots with Whatman no. 1 paper strips using 0.9% w/v NaCl solution as an eluent.

Animals

All experiments using animal models were approved by the Institutional Animal

Care and Use Committee at Seoul national university hospital, Seoul, Republic of Korea (Approval number:13-0265-COA1). Male balb/c mice, 10 - 16 wk. old, were purchased from Koatech. The mice were bred in the pathogen-free facility at Seoul national university hospital biomedical research institute. Weight-matched mice were housed in laboratory animal care facility in cages (5 mice /cage) and fed a standard diet.

In vivo micro SPECT/CT studies

7.4 – 14.8 MBq of ^{99m}Tc-HMPAO labeled NVs (n = 3) or 11.1 MBq of free ^{99m}Tc-HMPAO (n =1) were injected into the tail vein of the mice. At the 30min, 3 h, or 5 h after administration of ^{99m}Tc-HMPAO labeled NVs or ^{99m}Tc-HMPAO, serial SPECT/CT scan was acquired on a dedicated microSPECT/CT scanner (NanoSPECT/CT, Bioscan, Washington, DC). All mice were anesthetized and maintained with 1.5% isoflurane at 1 L/min oxygen flow and placed on the prone position under a scanner. The four multipinhole γ-detectors (9-pinholes) were used for high contrast collimation. Additional CT scans were acquired after SPECT acquisition for anatomical localization. Acquisition time was adjusted according to the counts to be more than 30,000 counts per projection. For SPECT images, 24 projections were acquired into a 512 × 512 acquisition matrix. The images were reconstructed by a 3-dimensional ordered-subsets expectation maximum (OSEM) algorithm. The radioactivity in the organs was calculated and compared with the

relative counts of the organs estimated in the SPECT images by region of interest (ROI) analysis. Data were expressed as percent of injected dose per gram (% ID/g).

Result

Radiolabeling NVs with ^{99m}Tc-HMPAO

Radiolabeling of NVs was performed with ^{99m}Tc-HMPAO by 1 h incubation at room temperature. After incubation, ^{99m}Tc-HMPAO or free ^{99m}Tc was removed by performed in two different methods. First method was based on size-exclusion based purification method using PD-10 column. In the elution group, 370 MBq ^{99m}Tc-HMPAO and 300 uL (90 μg) of NVs are used for radiolabeling. After incubation, elution was performed over PD-10 column using 0.9% w/v NaCl solution as an eluent. The each fraction was collected serially in test tube with the volume of 0.5 mL. Radioactivities of all test tubes were checked, and first peak was found in 6th test tube, indicating ^{99m}Tc-HMPAO labeled NVs. The providing specific activity of 6th tube was 132 μCi. The radiochemical purity determined by ITLC was 99.64%. In centrifugation method, initial dose of ^{99m}Tc-HMPAO was 185 MBq and 100 uL (30 ug) nanovesicles were used for labeling. After 1 h incubation at room temperature, the suspension was centrifuged with exosome spin column for 750xg 2 min. After centrifugation, the radio activity of product was 135 μCi, and radiochemical purity was checked as 93.73 ± 5.38% (Table 1)

Size distribution of ^{99m}Tc-HMPAO labeled NVs and free NVs

Particle size distribution of unlabeled NVs and ^{99m}Tc-HMPAO NVs was measured with dynamic light scattering (DLS). The result showed that the peak average diameter of ^{99m}Tc-HMPAO labeled NVs was 277.5 nm and 165.1 nm was checked for free NVs (Fig. 2). It reveals that particle size distribution of ^{99m}Tc-HMPAO labeled NVs was larger than those of free NVs.

Serum stability of ^{99m}Tc-HMPAO labeled NVs

Serum stability of ^{99m}Tc-HMPAO labeled NVs was investigated using human serum. The radiochemical purity of ^{99m}Tc-HMPAO labeled NVs was analyzed with ITLC at 10 min, 30 min, and 60 min after radiolabeling of NVs with ^{99m}Tc-HMPAO. ^{99m}Tc-HMPAO labeled NVs was stable in human serum with radiochemical purity of 94.8% and 90.6% after 10 min and 30 min, respectively. However, after 1 h radiochemical purity was checked as 70.2%, and after 3 h, the purity was lower than 50% (Fig. 3).

In vivo SPECT/CT studies of ^{99m}Tc-HMPAO labeled NVs and ^{99m}Tc-HMPAO

Biodistribution profiles of ^{99m}Tc-HMPAO-labeled NVs and ^{99m}Tc-HMPAO administrated intravenously was investigated by micro SPECT/CT in mice (Fig. 4). Within 30 min after injection, ^{99m}Tc-HMPAO labeled NVs were taken up mainly by the spleen and liver (liver: 26.9 ± 14.1, spleen: 21.8 ± 16.3). However, no significant brain uptake was observed, in contrast to the increased brain uptake of

^{99m}Tc-HMPAO treated mouse in 30 min image (6 %ID/g). This ^{99m}Tc-HMPAO labeled NVs uptake in liver and spleen slightly increased at 3 h and then slightly decreased at 5 h (Fig. 4B). In contrast, for ^{99m}Tc-HMPAO administrated mouse, initial increase of radioactivity was shown in the liver and spleen and then gradually decreased with relatively lower uptake (Fig. 4A). After 3 h, the increased uptake of ^{99m}Tc-HMPAO labeled NVs was found in salivary glands (16.7±0.9 %ID/g). For the ^{99m}Tc-HMPAO administrated mouse, increased brain (6 %ID/g) and salivary glands (5.3 %ID/g) uptakes were observed immediately after injection. The lung uptake was not observed in ^{99m}Tc-HMPAO labeled NVs administrated group until 5 h. However, for the ^{99m}Tc-HMPAO administrated mouse, lung uptake was observed right after injection. For the kidney, the maximum uptake observed at 3 h in ^{99m}Tc-HMPAO labeled NVs administrated group, in contrast to the immediate uptake and serial decrease of ^{99m}Tc-HMPAO treated mouse

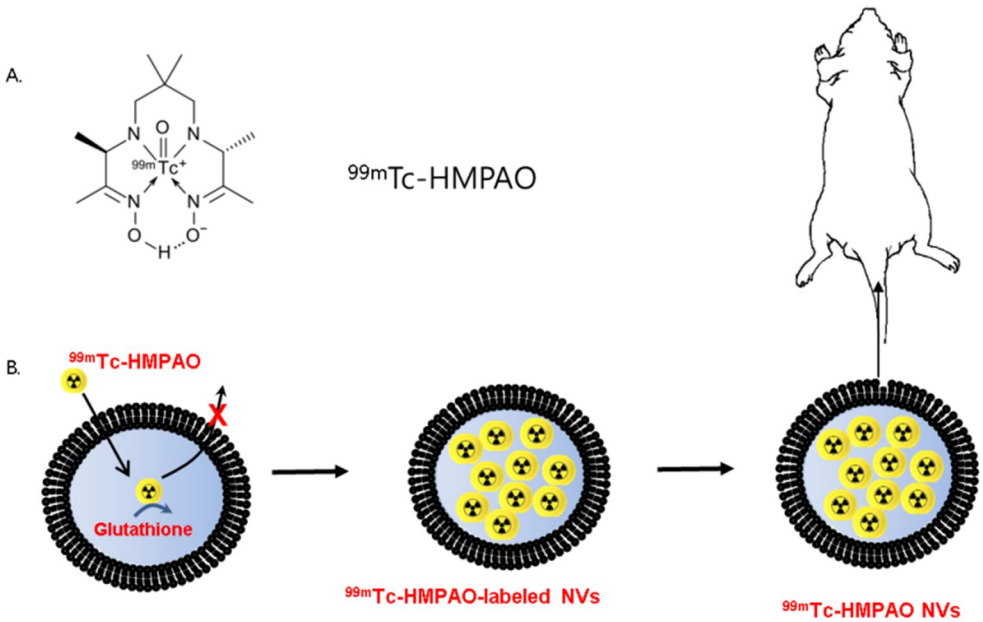

Figure 1. Schematic diagram of ^{99m}Tc-HMPAO trapping mechanism

A. Structure of ^{99m}Tc-hexamethylpropyleneamineoxime (HMPAO); B. Schematic diagram of ^{99m}Tc-HMPAO trapping mechanism. After lipophilic ^{99m}Tc-HMPAO enters the nanovesicle, it is converted to hydrophilic material by reaction with glutathione encapsulated in cell-derived nanovesicle.

Table 1. Radiochemical purity and duration of each isolation methods

*Procedure time: From the point of time which radiolabeling with ^{99m}Tc-HMPAO finished till end product production. Preparation times for PD-10 column or exosome spin column were excluded. ; **Radiochemical purity : Determined by ITLC using Whatman no. 1 paper and 0.9% w/v NaCl solution as an eluent.

Methods	*Procedure time	**Radiochemical purity (%)
Elution over PD-10 column	30 min	99.64
Centrifugation with exosome spin column	3 min	93.73 ± 5.38

A.

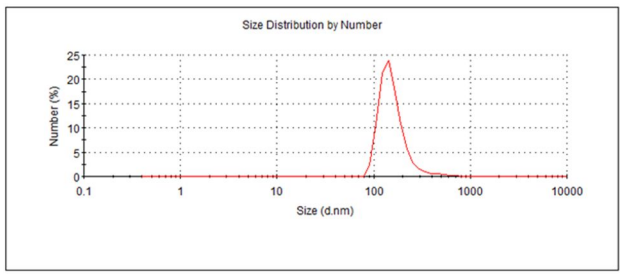

B.

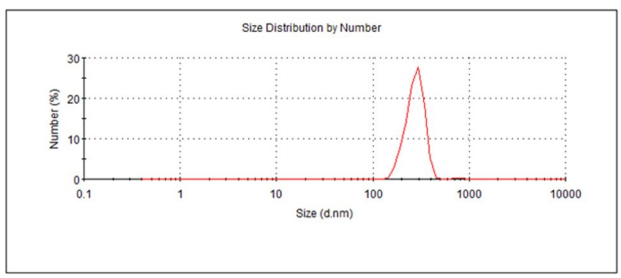

Figure 2. Size distributions of free nanovesicles (NVs) and ^{99m}Tc-HMPAO labeled NVs measured by the dynamic light scattering (DLS) technique. A. Average diameter of free NVs measured by DLS. The peak was checked as 165.1 nm; B. Average diameter of ^{99m}Tc-HMAPO labeled NVs measured by the DLS technique. The peak was checked as 277.5 nm

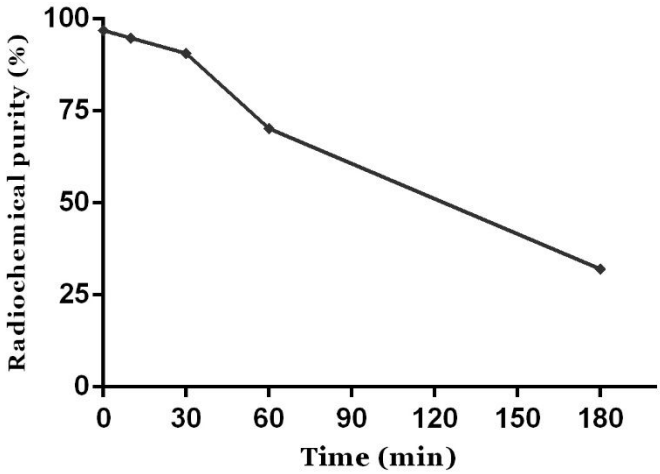

Figure 3. Serum stability of ^{99m}Tc-HMPAO labeled NVs in human serum.

The serum stability of ^{99m}Tc-HMPAO labeled NVs was analyzed by instant thin layered chromatography (TLC) using whatman No. 1 paper. The radiochemical purity was analyzed right after removing ^{99m}Tc-HMPAO by centrifugation with exosome spin column. Initial radiochemical purity of ^{99m}Tc-HMPAO labeled NVs was more than 95%**.** ^{99m}Tc-HMPAO labeled NVs is stable in human serum until 30 min with more than 90% radiochemical purity. But serum stability was decreased after 1 h, with about 70% of radiochemical purity.

A.

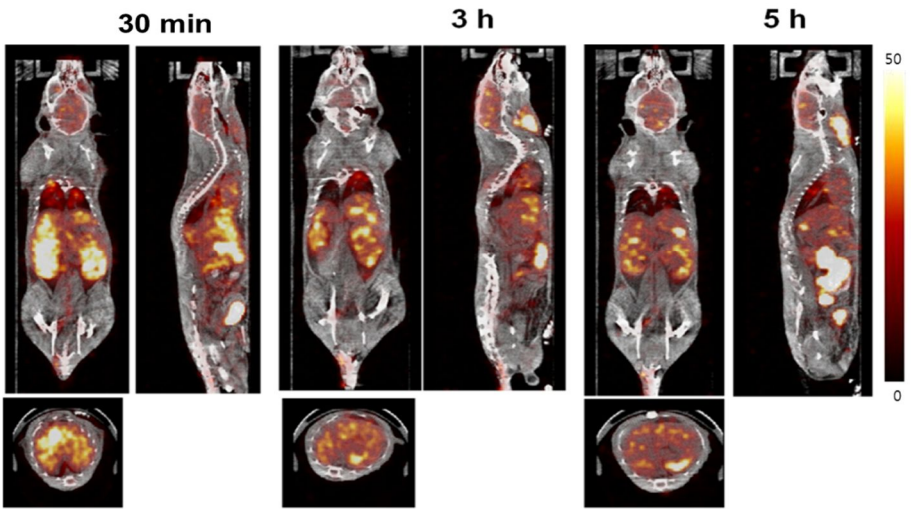

B.

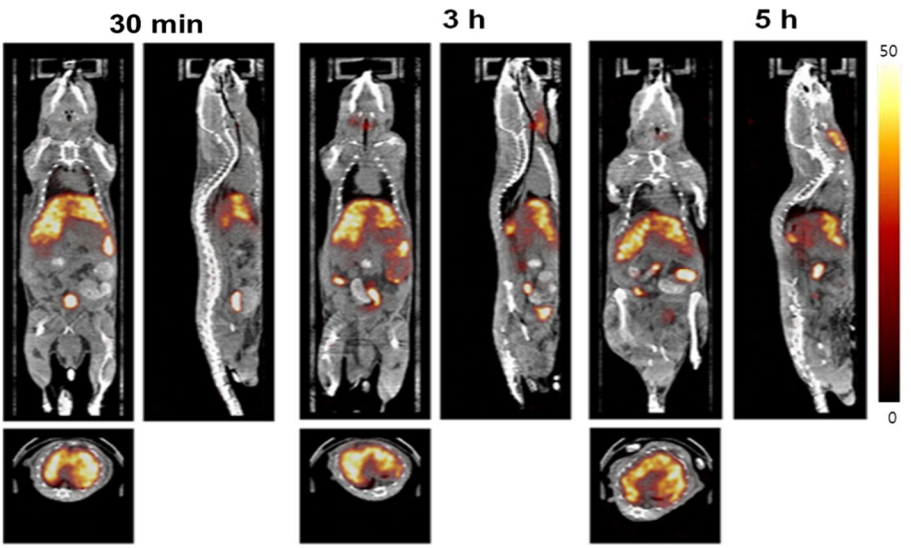

Figure 4. Comparison of serial *in vivo* SPECT/CT images after ^{99m}Tc-HMPAO or ^{99m}Tc-HMPAO labeled NVs administration in mice. A. Serial SPECT/CT images acquired at 30 min, 3 h, and 5 h post administration of ^{99m}Tc-HMPAO B. Serial SPECT/CT images acquired at 30 min, 3 h, and 5 h post administration of ^{99m}Tc-HMPAO labeled NVs in mouse. The 3-dimensional reconstruction of the single-photon emission computed tomography with CT (SPECT/CT) showed early increased activity of brain and salivary glands in ^{99m}Tc-HMPAO administrated mouse (A), contrast to ^{99m}Tc-HMPAO labeled NVs administrated mouse (B) showing delayed salivary glands uptake and no significant brain activity.

A.

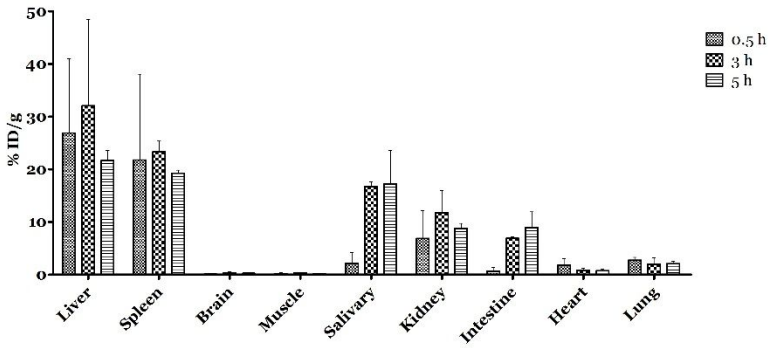

B.

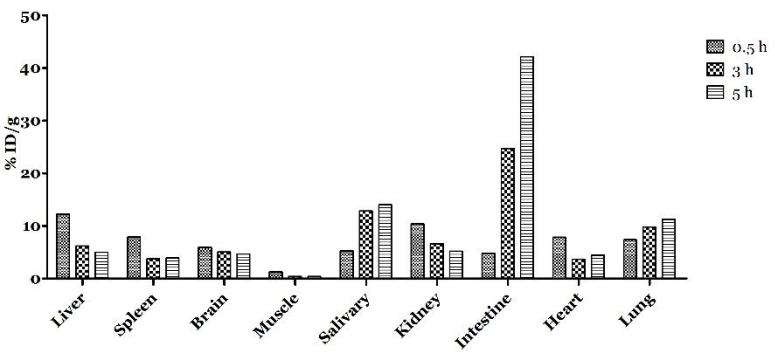

Figure 5. Image based biodistribution analysis of ^{99m}Tc-HMPAO labeled NVs and ^{99m}Tc-HMPAO analyzed with SPECT/CT scan.

Serial SPECT/CT images were analyzed to determine %ID/g for biodistribution of ^{99m}Tc-HMPAO labeled NVs (A; n = 3), and biodistribution of ^{99m}Tc-HMPAO (B; n = 1). Liver and spleen show 2-3 folds higher ^{99m}Tc-HMPAO labeled NVs uptake than ^{99m}Tc-HMPAO, but no significant ^{99m}Tc-HMPAO labeled NVs uptake in brain was observed in contrast to ^{99m}Tc-HMPAO uptake in brain. Data are presented as mean ± S.D. for ^{99m}Tc-HMAPO labeled NVs

Discussion

Exosome has been proposed as an alternative drug delivery vehicle to reduce the side effect and deliver high dose of drug to target specific organ (15). Especially, dendritic cell derived exosome is reported to target inflammatory or cancerous condition (7, 16). However most previous reports have been studied the targeted delivery of exosome by fluorescence (8, 17, 18). So far, there was no study which attempts to visualize biodistribution of exosome *in vivo*. For the clinical application as a various drug delivery vehicle, *in vivo* biodistribution study of exosome is essential.

Therefore, for the *in vivo* biodistribution investigation, we introduced ^{99m}Tc-HMPAO as a potential radioligand for radiolabeling of the exosome. By reaction with sulfhydryl groups of the glutathione encapsulated inside cells, ^{99m}Tc-HMPAO became hydrophilic compounds and easily trapped within cell. Because of this property, ^{99m}Tc-HMPAO is widely used for labeling mammalian cells, especially for the WBC scan for clinical use (19). In this study, exosome-mimetic nanovesicle were used that presents similar feature to exosome, and that has 100-folds higher yield than natural exosome (7). Radiolabeling of this NVs with ^{99m}Tc-HMPAO was successfully performed and radiochemical purity was more than 95% after removing of ^{99m}Tc-HMPAO. However, the crucial problem was loss of NVs during removing process of ^{99m}Tc-HMPAO. We compared two separation methods, and

both methods of size-exclusion column showed excellent radiochemical purity, but large amount of NVs loss are observed during elution over PD-10 column. And the method of PD10-based elution takes longer separation time than filter-based centrifugation, about 15 times (30 min vs 3 min, Fig. 1). Although there is a limitation because of small volume of exosome spin column, we suggest that exosome filter based centrifugation would be a better method of nanovesicle isolation for clinical use.

After radiolabeling, serum stability was checked in human serum. ^{99m}Tc-HMPAO labeled NVs were stable in human serum up to 90% at 30 min after administration to human serum. However, after 1 h, radiochemical purity was decreased to 70%. Further study should be performed to identify mechanism of instability after 1 h. It could be due to the degradation of ^{99m}Tc-HMPAO labeled NVs after administration into human serum or just ^{99m}Tc-HMPAO getting out from the nanovesicles as time passed.

In vivo SPECT/CT imaging after ^{99m}Tc-HMPAO labeled NVs administration, at the 30 min image, most of the uptakes are observed in liver and spleen, about 2-3 folds higher than ^{99m}Tc-HMPAO administrated mouse (Fig. 5). In previous several studies, nanoparticles of 150-300 nm are captured mainly in the liver and the spleen (20). The higher uptake of liver and spleen which observed in ^{99m}Tc-HMPAO-labeled NVs administrated group could be a result of phagocytosis of radiolabeled nanovesicles, by immune cells in reticuloendothelial system of liver

and spleen. The distribution of ^{99m}Tc-HMPAO NVs investigated by SPECT/CT is comparable to similar size nanomaterial biodistribution (21). Brain uptake was not observed in ^{99m}Tc-HMPAO labeled NVs administration group, in contrast for ^{99m}Tc-HMPAO administrated mice, the increased uptake was observed in the brain corresponding to previous study (22). Therefore, we can suggest radiolabeling of NVs was performed successfully, and at least within 30 min, dissociation of ^{99m}Tc-HMPAO were not occurred. After 3 h of administration, brain uptakes are still not observed. However salivary glands uptake were appeared 30 min after administration and increased as time passed. This salivary glands activity might be a result of metabolite of ^{99m}Tc-HMPAO uptake of parotid gland (23). According to previous study, ^{99m}Tc-HMPAO was unstable in serum and rapidly breakdown in blood (22). Because of this instability, uptake of salivary gland could be result of metabolite of ^{99m}Tc-HMPAO uptake after NV's degradation. And this result is consistent with our serum stability analysis result. Reason of ^{99m}Tc-HMPAO metabolite release from NVs is not clear. It could be result of nanovesicle degradation by hepatocyte or RES of spleen or just because of ^{99m}Tc-HMPAO metabolite released from NVs by unclear mechanism. Additional studies should be needed for evaluating this mechanism.

In this study we evaluated the possibility of *in vivo* imaging of NVs using ^{99m}Tc-HMPAO radiolabeling. This study is the first attempt to investigate *in vivo* distribution of cell-derived NVs which was impossible with conventional methods,

such as fluorescence. And with this approach, using ROI analysis, we can quantify the organ uptake of NVs. However, there is several limitations of this study. Firstly, characterization of NVs after radiolabeling was investigated with dynamic light scattering only. We are also planning additional studies such as transmission electron microscope (TEM) image and protein assay to characterization of nanovesicles after radiolabeling. Secondly, the imaging of ^{99m}Tc-HMPAO administration was just performed in one mouse. Therefore it was difficult to perform statistical significance test between ^{99m}Tc-HMPAO labeled NVs administration group and ^{99m}Tc-HMPAO administration group. However, biodistribution of ^{99m}Tc-HMPAO is well identified already, and our data of ^{99m}Tc-HMPAO biodistribution measured by SPECT/CT showed consensus with previous study (24). Therefore the difference between biodistribution of two groups could be acceptable. However, as I mentioned previously, the mechanism of ^{99m}Tc-HMPAO dissociation from NVs after 3 h is not clear. Future plan is to make additional experiments for investigating *in vivo* stability of radiolabeled nanovesicles, and investigate the radiolabeled NVs to animal model to target inflammatory or cancerous condition for biological application.

Conclusion

Exsosome-mimetic NVs was successfully radiolabeled with ^{99m}Tc-HMPAO for small animal *in vivo* imaging of SPECT/CT scan. It might be a useful method for *in vivo* biodistribution study of exosome mimetic NVs.

Reference

1.Denzer K, Kleijmeer MJ, Heijnen HF, Stoorvogel W, Geuze HJ. Exosome: from internal vesicle of the multivesicular body to intercellular signaling device. J Cell Sci. 2000 Oct;113 Pt 19:3365-74.

2.Camussi G, Deregibus MC, Bruno S, Cantaluppi V, Biancone L. Exosomes/microvesicles as a mechanism of cell-to-cell communication. Kidney Int. 2010 Nov;78:838-48.

3.van Dommelen SM, Vader P, Lakhal S, Kooijmans SA, van Solinge WW, Wood MJ, et al. Microvesicles and exosomes: opportunities for cell-derived membrane vesicles in drug delivery. J Control Release. 2012 Jul 20;161:635-44.

4.Ohno S, Takanashi M, Sudo K, Ueda S, Ishikawa A, Matsuyama N, et al. Systemically injected exosomes targeted to EGFR deliver antitumor microRNA to breast cancer cells. Mol Ther. 2013 Jan;21:185-91. PubMed PMID: 23032975.

5.Segura E, Nicco C, Lombard B, Véron P, Raposo G, Batteux F, et al. ICAM-1 on exosomes from mature dendritic cells is critical for efficient naive T-cell priming. Blood. 2005;106:216-23.

6.Théry C, Amigorena S, Raposo G, Clayton A. Isolation and characterization of exosomes from cell culture supernatants and biological fluids. Current Protocols in Cell Biology. 2006:3.22. 1-3.. 9.

7.Jang SC, Kim OY, Yoon CM, Choi DS, Roh TY, Park J, et al. Bioinspired exosome-mimetic nanovesicles for targeted delivery of chemotherapeutics to

malignant tumors. ACS Nano. 2013 Sep 24;7:7698-710.

8.Haney MJ, Zhao Y, Harrison EB, Mahajan V, Ahmed S, He Z, et al. Specific transfection of inflamed brain by macrophages: a new therapeutic strategy for neurodegenerative diseases. PLoS One. 2013;8:e61852.

9.Parolini I, Federici C, Raggi C, Lugini L, Palleschi S, De Milito A, et al. Microenvironmental pH is a key factor for exosome traffic in tumor cells. The Journal of biological chemistry. 2009 Dec 4;284:34211-22.

10.Singh R, Pantarotto D, Lacerda L, Pastorin G, Klumpp C, Prato M, et al. Tissue biodistribution and blood clearance rates of intravenously administered carbon nanotube radiotracers. Proceedings of the National Academy of Sciences of the United States of America. 2006;103:3357-62.

11.Kumar R, Roy I, Ohulchanskky TY, Vathy LA, Bergey EJ, Sajjad M, et al. In vivo biodistribution and clearance studies using multimodal organically modified silica nanoparticles. ACS nano. 2010;4:699-708.

12.Lee KJ, Hahm KB, Kim YS, Kim JH, Cho SW, Jie H, et al. The usefulness of Tc-99m HMPAO labeled WBC SPECT in eosinophilic gastroenteritis. Clin Nucl Med. 1997 Aug;22:536-41.

13.Rypins EB, Evans DG, Hinrichs W, Kipper SL. Tc-99m-HMPAO white blood cell scan for diagnosis of acute appendicitis in patients with equivocal clinical presentation. Ann Surg. 1997 Jul;226:58-65.

14.Hamilton G. A simple method of producing diagnostic copies from overexposed

radiographs. Can Assoc Radiol J. 1991 Jun;42:216-8.

15.Lakhal S, Wood MJ. Exosome nanotechnology: an emerging paradigm shift in drug delivery: exploitation of exosome nanovesicles for systemic in vivo delivery of RNAi heralds new horizons for drug delivery across biological barriers. Bioessays. 2011 Oct;33:737-41.

16.Sun DM, Zhuang XY, Xiang XY, Liu YL, Zhang SY, Liu CR, et al. A Novel Nanoparticle Drug Delivery System: The Anti-inflammatory Activity of Curcumin Is Enhanced When Encapsulated in Exosomes. Molecular Therapy. 2010 Sep;18:1606-14.

17.Tian Y, Li S, Song J, Ji T, Zhu M, Anderson GJ, et al. A doxorubicin delivery platform using engineered natural membrane vesicle exosomes for targeted tumor therapy. Biomaterials. 2014;35:2383-90.

18.Pegtel DM, Cosmopoulos K, Thorley-Lawson DA, van Eijndhoven MA, Hopmans ES, Lindenberg JL, et al. Functional delivery of viral miRNAs via exosomes. Proceedings of the National Academy of Sciences. 2010;107:6328-33.

19.Kelbaek H, Linde J, Nielsen SL. Evaluation of a new leukocyte labeling procedure with 99mTc-HMPAO. Eur J Nucl Med. 1988;14:621-3.

20.Gaumet M, Vargas A, Gurny R, Delie F. Nanoparticles for drug delivery: the need for precision in reporting particle size parameters. European Journal of Pharmaceutics and Biopharmaceutics. 2008;69:1-9.

21.Kunzmann A, Andersson B, Thurnherr T, Krug H, Scheynius A, Fadeel B.

Toxicology of engineered nanomaterials: focus on biocompatibility, biodistribution and biodegradation. Biochimica et Biophysica Acta (BBA)-General Subjects. 2011;1810:361-73.

22.Lucignani G, Rossetti C, Ferrario P, Zecca L, Gilardi MC, Zito F, et al. In vivo metabolism and kinetics of ^{99m}Tc-HMPAO. Eur J Nucl Med. 1990;16:249-55.

23.Helman J, Turner R, Fox PC, Baum BJ. ^{99m}Tc-pertechnetate uptake in parotid acinar cells by the Na+/K+/Cl-co-transport system. Journal of Clinical Investigation. 1987;79:1310.

24.Nakamura K, Tukatani Y, Kubo A, Hashimoto S, Terayama Y, Amano T, et al. The behavior of ^{99m}Tc-hexamethylpropyleneamineoxime (^{99m}Tc-HMPAO) in blood and brain. European journal of nuclear medicine. 1989;15:100-7

요약 (국문초록)

소동물 SPECT/CT를 이용한 ^{99m}Tc-HMPAO을 표지 한 엑소좀 모방 나노 소포체의 생체 내 분포 모니터링

유민영

WCU, 분자의학 및 바이오제약학과

융합과학기술대학원

서울대학교

목적:

엑소좀의 대안으로 개발 된 엑소좀 모방 나노 소포체는 최근 유망한 약물 전달 체로서 주목 받고 있다. 이 나노 소포체의 생체 내 에서의 분포는 약물 전달 체로서의 역할에 중요한 영향을 미치기 때문에 매우 중요하다. 그러나 최근까지 이러한 나노 소포체의 생체 내 분포연구는 형광 기반의 접근 방식에 한정되었고, 이러한 방법은 인체에 적용시켜 시각화 하기엔 본질적 어려움이 있었다. 따라서 이 연구에서, 우리는 대식세포 유래 나노 소포체에 간단한 표지 방법으로 친 유성 방사성 추적자인 ^{99m}Tc-hexamethylpropyleneamineoxime (HMAPO)을 표지 하여 생쥐에 주사 후 소동물 SPECT / CT 영상을 통해 생체 내 나노 소포체의 분포를 분석하였다.

방법:

나노 소포체는 생쥐의 RAW 264.7 대식세포를 분쇄 후 단계적으로 걸러내어 생산하였다(10, 5, and 1 μm). 나노 소포체의 표지는 실온에서 1 시간 동안

^{99m}Tc-HMPAO와 반응시킨 후 유리 ^{99m}Tc-HMPAO 를 PD-10 column을 통한 용리 혹은 exosome spin column을 이용한 원심분리로 수행하였다. 이후 사람 혈청을 이용하여 표지 한 지 10분, 30분, 1시간 및 3시간째에 혈청 내 안정성을 확인하였다. 나노 소포체의 생체 내 분포를 확인하기 위하여 ^{99m}Tc-HMPAO 표지 된 나노 소포체 및 ^{99m}Tc-HMPAO를 생쥐에 주사 후 SPECT/CT를 30분, 3시간 및 5시간째에 촬영하여 분석하였다.

결과:

한 시간 동안 나노 소포체와 ^{99m}Tc-HMPAO 와 반응 시킨 후 PD-10 column을 통한 용리 혹은 exosome spin column을 이용하여 유리 ^{99m}Tc-HMPAO를 제거한 후 TLC로 측정한 radiochemical purity는 99.64% 및 93.73 ± 5.38% 였다. ^{99m}Tc-HMPAO 표지 된 소포는 혈청 내에서 30분 내에 90% 이상의 안정성을 보였으나, 1시간 이후에는 70% 정도로 감소되었다. 생체 내 분포의 평가를 위한 SPECT/CT에서는 ^{99m}Tc-HMPAO 표지 나노 소포체와 ^{99m}Tc-HMPAO가 확연하게 다른 분포를 보였다. 표지 된 나노 소포체의 간 섭취가 ^{99m}Tc-HMPAO에 비하여 확연히 높은 것이 확인 되었으며, 상대적으로 낮은 섭취가 심장 및 침샘에서 관찰되었다. ROI를 통한 정량적인 분석에서, 간 및 비장에서의 섭취가 총 주사량의 50% 이상을 차지하는 것이 확인 되었다.

결론:

이 연구에서는 ^{99m}Tc-HMPAO 표지 나노 소포체의 생체 내 분포를 SPECT/CT를 통해 정량적으로 분석하였다. 이번 연구에서 이용한 방사성 표지

된 나노 소포체를 통해 엑소좀을 이용한 약물전달 시스템에 대한 이해 향상 및 향후의 이용에 도움을 줄 수 있을 것으로 기대한다.

keywords: 엑소좀, ^{99m}Tc-HMPAO, 방사성 동위원소 표지
Student Number: 2012-24149